Environmental Research 185 (2020) 109451

Contents lists available at ScienceDirect

Environmental Research

journal homepage: www.elsevier.com/locate/envres

Bacterial response mechanism during biofilm growth on different metal material substrates: EPS characteristics, oxidative stress and molecular regulatory network analysis

Jiaping Wang, Guiying Li, Hongliang Yin, Taicheng An*

Guangdong Key Laboratory of Environmental Catalysis and Health Risk Control, Guangzhou Key Laboratory Environmental Catalysis and Pollution Control, School of Environmental Science and Engineering, Institute of Environmental Health and Pollution Control, Guangdong University of Technology, Guangzhou, 510006, China

ARTICLE INFO

Keywords:
Bacterial biofilm
Growth profiles
EPS
Oxidative stress
Metal-based pipeline materials

ABSTRACT

Overwhelming growth of bacterial biofilms on different metal-based pipeline materials are intractable and pose a serious threat to public health when tap water flows though these pipelines. Indeed, the underlying mechanism of biofilm growth on the surface of different pipeline materials deserves detailed exploration to provide subsequent implementation strategies for biofilm control. Thus, in this study, how bacteria response to their encounters was explored, when they inhabit different metal-based pipeline substrates. Results revealed that bacteria proliferated when they grew on stainless steel (SS) and titanium sheet (Ti), quickly developing into bacterial biofilms. In contrast, the abundance of bacteria on copper (Cu) and nickel foam (Ni) substates decreased sharply by 4–5 logs within 24 h. The morphological shrinkage and shortening of bacterial cells, as well as a sudden 64-fold increase of carbohydrate content in extracellular polymeric substances (EPS), were observed on Cu substrate. Furthermore, generation of reactive oxygen species and fluctuation of enzymatic activity demonstrated the destruction of redox equilibrium in bacteria. Bacteria cultured on Cu substrate showed the strongest response, followed by Ni, SS and Ti. The oxidative stress increased quickly during the growth of bacterial biofilm, and almost all tested metal transporter-related genes were upregulated by 2–11 folds on Cu, which were higher than on other substrates (1–2 folds for SS and Ti, 2–9 folds for Ni). Finally, these behaviors were compared under the biofilm regulatory molecular network. This work may facilitate better understanding different response mechanisms during bacterial biofilm colonization on metal-based pipelines and provide implications for subsequent biofilm control.

1. Introduction

The occurrence of bacteria in drinking water is undesirable due to their potential risks to human beings. However, bacteria overwhelmingly live as biofilms, which are one of the most common and successful forms of life on earth, and are found on almost all natural and artificial surfaces (Flemming et al., 2016; Nakano and Strayer, 2014; Stewart and Franklin, 2008; Vlamakis et al., 2013). Aggregations of bacteria are embedded in the extracellular matrix secreted by themselves to form biofilms (Flemming et al., 2016). Bacteria in aqueous systems prefer to sticking on substrate surfaces and many negative effects of this tendency are becoming increasingly prominent as compared with their planktonic form. Water distribution systems for drinking water, industrial pipelines, air conditioning systems and hospitals are common places where biofilm bacteria colonize, blocking corrosion of industrial equipment (Shivapooja et al., 2013), deterioration of drinking water quality (Isaac and Sherchan, 2020; Liu et al., 2016), and causing medical infections (Flemming and Wingender, 2010).

Why have biofilm formation and surface binding become such a common phenomenon? What is the mechanism behind it? Generally, the surface of a substrate provides a space where bacteria can steadily grow. Furthermore, surface colonization can also concentrate nutrients (Hall-Stoodley et al., 2004). That is, biofilm bacteria can adjust biofilm structure through mass transfer to enter a local growth mode under capricious environmental conditions, which ensures flexibility to adapt quickly (Markova et al., 2018). Importantly, the of biofilm formation provides protection for the internal bacteria under harsh environments, including metal toxicity, acid exposure, dehydration, salinization, antibiotics and disinfectants (Hall-Stoodley et al., 2004; Xiao et al., 2016; Zhang et al., 2015). Intuitively, extracellular polymeric substance (EPS) matrix in biofilm can reasonably represent a diffusion barrier. By

* Corresponding author.
E-mail address: antc99@gdut.edu.cn (T. An).

https://doi.org/10.1016/j.envres.2020.109451
Received 16 November 2019; Received in revised form 7 February 2020; Accepted 26 March 2020
Available online 01 April 2020
0013-9351/

reducing the effective bactericidal concentration to a sublethal concentration, the EPS inhibits antimicrobial agent diffusion, while sublethal doses of bactericides can induce a more tolerant phenotype (Flemming et al., 2016). Moreover, slow growth and dormancy of bacteria have long been recognized as means by which bacteria can survive in biofilms when exposed to antibiotics. Slow growth can drive bacteria into a dormant form, but metabolic activity and membrane integrity remain unchanged throughout the dormancy (Chen et al., 2018; Lewis, 2007).

Surfaces of many objects, including drinking water distribution pipelines, industrial equipment and medical devices, have become havens for biofilms and could pose a major public health threat. Rather, the formation mechanism of biofilms from planktonic cells is still under the spotlight and intensely debated. Moreover, the impact of biofilm formation and propagation on the safety of drinking water supplies is still seriously concerning. Therefore, exploring and understanding the underlying mechanisms that occur during the biofilm formation process, i.e. attachment of planktonic bacteria to the surface of a material, are crucial to identifying a control strategy.

The majority of pipeline networks are iron-(stainless steel and galvanized steel) or copper-based materials (Liu et al., 2016). It has been reported that although many biofilm bacteria favor iron-based pipes to copper pipes (Jungfer et al., 2013; Ren et al., 2015), some bacteria still aggregate on the surface of copper pipes used in both municipal and household settings (Buse et al., 2017; Proctor et al., 2017). Correspondingly, during the biofilm formation process, metals can cause discrete and distinct injury to microbial cells as a result of oxidative stress, protein dysfunction or membrane damage (Lemire et al., 2013; Santo et al., 2011; Warnes et al., 2012). These phenomena are also very similar to the state of planktonic bacteria as they are subjected to inactivation (Sun et al. 2014, 2016), suggesting that biofilm bacteria may also have such an inactivation mechanism when in contact with metal substrates and some materials could inhibit biofilm development.

Nevertheless, many questions still need to be answered. For example, are metal ions also released from different substrates during the biofilm formation process? What do biofilm bacteria produce to fight them? In this context, is the secreted EPS acted as a strong shelter to reduce the growth rate and energy consumption, allowing for local growth through sacrifice and energy transfer? Moreover, when bacteria are not completely inactivated, what is the process of bacterial survival and what is the mechanism behind it? How does this differ from the normal bacterial colonization process on the surface of different substrates? In a word, the whole formation process of bacterial biofilms and the underlying response mechanisms have not been clearly explored and explained.

Therefore, this work mainly aimed to answer the above questions. For this purpose, a model bacterial strain, *Escherichia coli* K-12, was used for microbial growth and biofilm formation experiments. Four kinds of metals (stainless steel, copper, titanium and nickel) that are used for pipelines or are otherwise extensively used as materials were selected as substrates. Visualization and evaluation of biofilm morphology and thickness were first performed using scanning electron microscopy (SEM) and 3D image reconstruction with a confocal laser scanning microscope (CLSM). Furthermore, EPS was extracted and quantified, and the intracellular reactive oxygen species (ROSs) were detected. Superoxide dismutase (SOD), catalase (CAT) and glutathione peroxidase (GSH-Px) activities were also measured to indicate antioxidant activities during biofilm formation. Real-time polymerase chain reaction (qPCR) was used to quantify the expression of genes involved in oxidative stress regulation, metal transporter and different regulatory mechanisms of biofilm formation. This work could facilitate a better understanding of the different strategies pursued by biofilm bacteria when colonizing metal-based pipelines, thereby providing a control and elimination strategy for biofilms in water distribution systems.

2. Materials and methods

2.1. Substrate material characterization

The experiment selected 304 stainless steel sheet (SS), copper sheet (Cu), titanium sheet (Ti) and nickel foam (Ni) were all from Congyuan Instrument co., Guangzhou, China, as biofilm growth substrates. The surface morphology of these materials was imaged (Fig. S1) using high-resolution SEM (SU8010, Hitachi, Japan). Material composition was characterized using X-ray diffraction (Rigaku Co., Japan) and all the diffraction peaks were perfectly directed to the materials (Fig. S2).

2.2. Bacterial incubation and biofilm development

Bacterial incubation procedure was similar to the typical procedure described previously (Chen et al., 2019; Li et al., 2020). Briefly, *E. coli* K-12 (Coli Genetic Stock Center, Yale University, New Haven, CT, USA) was plated from frozen stock on nutrient agar and incubated at 37 °C. A single bacterial colony was picked and incubated overnight in Luria-Bertani (LB) broth at 37 °C. After centrifugation at 8000 rpm for 2 min, the bacterial pellet was resuspended in M9 Minimal Medium (Sangon Biotech Co., China) and then diluted to a concentration of 10^9 colony forming units per milliliter (CFU ml^{-1}).

The biofilm was cultured in a multi-channel biofilm flow chamber (Fig. S3) at room temperature (O'Toole et al., 1999, Tolker-Nielsen et al., 2014). Briefly, the sterilized metal material was placed in a flow chamber and then 200 μL of bacterial suspension was added to the surface of the material and left for 3 h to allow for attachment. A peristaltic pump was used to feed the M9 culture solution into the reactor at a flow rate of 0.4 mL per minute per channel. The growth curve of the bacterial biofilm on each material was determined to assess viability and potential growth throughout the experiment.

2.3. Evaluation of thickness during biofilm development

Visualization and evaluation of biofilm thickness was done through 3D image reconstruction using the CLSM Z–stacks function (LSM-800, Carl Zeiss, Germany) according to previous reference (Lee et al., 2018). Biofilm samples were stained with ofloxacin (intrinsically fluorescent antibiotic) for CLSM image analysis (excitation wavelength: 405 nm) (Stone et al., 2018). Mutual matching of bacterial images in bright and dark fields verified that ofloxacin entered bacterial cells and the staining was successful (Fig. S4). Biofilm samples from the flow chamber at designated times were scraped, mounted on polylysine glass slides and then stained with ofloxacin solution. After 20 min incubation, samples were immersed in fresh phosphate buffered solution (PBS) to remove excess dye. The biofilm samples were then dried and sealed for testing. The entire ofloxacin treatment procedure for CLSM analysis was completed within 3 h.

2.4. SEM sample preparation

Images were obtained at different biofilm growth stages. Surface floating bacteria were gently washed away three times with PBS. After fixation and dehydration, samples were freeze-dried, sprayed with gold and then observed by SEM (SU8010, Hitachi, Japan).

2.5. Extraction and determination of EPS

Biofilms were sampled at different biofilm growth stages, bathed at 60 °C for 40 min and then cooled. After reaching ambient temperature (23 ± 2 °C), the biofilm and PBS mixtures were transferred into 1.5-mL tubes and then centrifuged at 4000 rpm for 20 min. EPS extracts were filtered using 0.45 μm nylon membranes (Perez and Susa, 2017). Total protein concentration of the EPS extracts was determined using a modified Lowry Protein Assay Kit (Pierce Biotechnology, USA) with

bovine serum albumin as a standard. Total polysaccharide concentration was determined by phenol-sulfuric acid method using glucose as a standard.

2.6. ROS detection and enzymatic activity assays

Intracellular ROSs were quantified using the fluorogenic dye 2′7′-dichlorofluorescein diacetate (DCFH-DA) (Invitrogen, Carlsbad, USA). The production levels of ROSs from different biofilm materials were normalized to that of the control sample at the initial time. SOD, CAT and GSH-Px activities were analyzed to determine antioxidant activity. Details of all assay procedures are summarized in the Supporting Information.

2.7. Assessment of mRNA gene expression

Total RNA from bacterial biofilms on different materials was obtained using a bacterial total RNA extraction kit (Sangon Biotech Co., China). The subsequent cDNA was synthesized by M-MLV Reverse Transcription Kit (Invitrogen Inc., USA). The qPCR was used to quantify the gene expression of various functions. The primers used in this study are listed in Table S1. Detailed information about the genes and reaction procedures for the qPCR are provided in Supporting Information.

2.8. Statistical analysis

Measurements of EPS, ROSs and enzymatic activities of bacterial biofilms on different materials were conducted three times. Results are expressed as mean ± standard deviation. The laser confocal image Z-axis data and image pixels were converted to 3D and the parameters were analyzed using quantitative software (Imaris version 8.3, Bitplane AG, Zurich, Switzerland) according to reference (Azeredo et al., 2017).

3. Results and discussion

3.1. Growth activity of bacterial biofilms on different substrates

To evaluate the bacterial growth activity on different substrates, the growth curves of *E. coli* K-12 on the substrates (SS, Ti, Cu and Ni) were determined. The biofilm formation processes were different for these metal substrates (Fig. 1a1 and 1a2), as determined using plate colony-counting method. On SS and Ti substrates, the bacterial abundance first increased gradually with cultivation time, then remained constant, and finally decreased gradually, indicating that the biofilm bacteria could better adapt to the surface of these substrates. A slight difference between the two substrates was that the biofilm bacteria on SS grew faster at first and then decreased faster afterwards. The decreased amount of biofilm indicates that the growth of the biofilm reached the shedding stage. The bacterial abundance on SS decreased faster than that on Ti, indicating that the bacteria could adapt to SS faster and the biofilm growth cycle was shorter. Comparatively, on Cu and Ni substrates, the bacterial number decreased sharply at the beginning of cultivation (within 24 h) by 4–5 logs and then gradually increased, reaching 5.1×10^8 and 3.9×10^8 CFU mL^{-1}, respectively, within 48 h. Finally, the bacterial abundance leveled off. This indicates that the bacteria did not adapt well on Cu and Ni substrates at first, as compared with SS and Ti substrates; however, this incompatibility changed during bacterial biofilm development.

These results were confirmed using CLSM analysis (Fig. S5) by quantifying the biofilm thickness. The biofilm thickness increased gradually and then decreased during the 96-h biofilm formation process on all substrates except Ni (Fig. 1b). This indicates that the biofilms gradually developed and that the biofilms on SS, Ti, and Cu substrates were at the biofilm dispersion stage after 84-h cultivation, while biofilm on Ni had not yet reached the dispersion stage. Further research has found that trends in biofilm thickness were different from that of

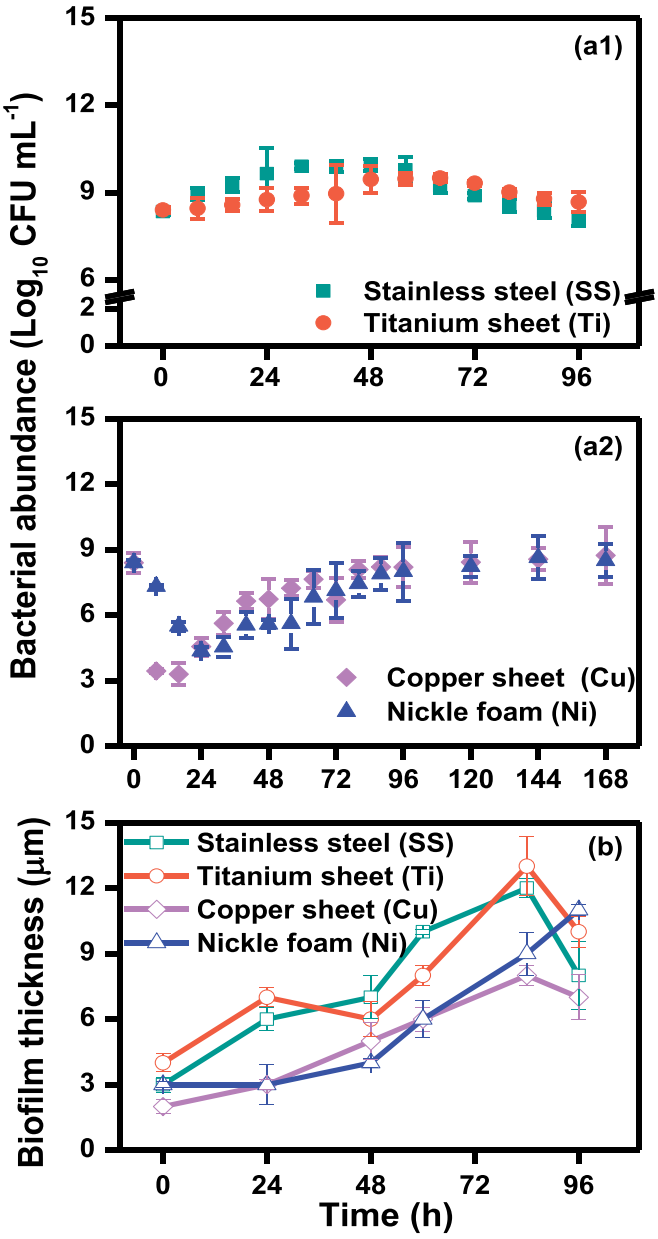

Fig. 1. Biofilm development and cell proliferation (a1 and a2) and biofilm thickness (b) of *E. coli* K-12 evaluated using plate colony-counting method and CLSM, respectively.

bacterial abundance. For instance, on Cu and Ni substrates, although the bacterial abundance decreased quickly during the initial period, the biofilm thickness increased gradually until it reached a stable thickness. The reason for this is that during bacterial biofilm development, biofilms not only consists of bacteria, but also self-produced EPS (Flemming and Wingender, 2010). This can also explain the different trends in bacterial abundance and biofilm thickness.

Obviously, the biofilm formation performance of the bacteria on different materials was distinct. The initial bacterial growth activities on Cu and Ni substrates were much lower than those on SS and Ti, which might be due to the distinct interactions of bacteria with different materials. For instance, during cultivation process, a green substance was formed on the Cu surface (Fig. S6). It is likely that Cu surface is oxidized to copper ions, which releases and then hinders cellular protein or enzyme activity, thereby effectively preventing planktonic bacteria from attaching to Cu substrate surface (Santo et al., 2011).

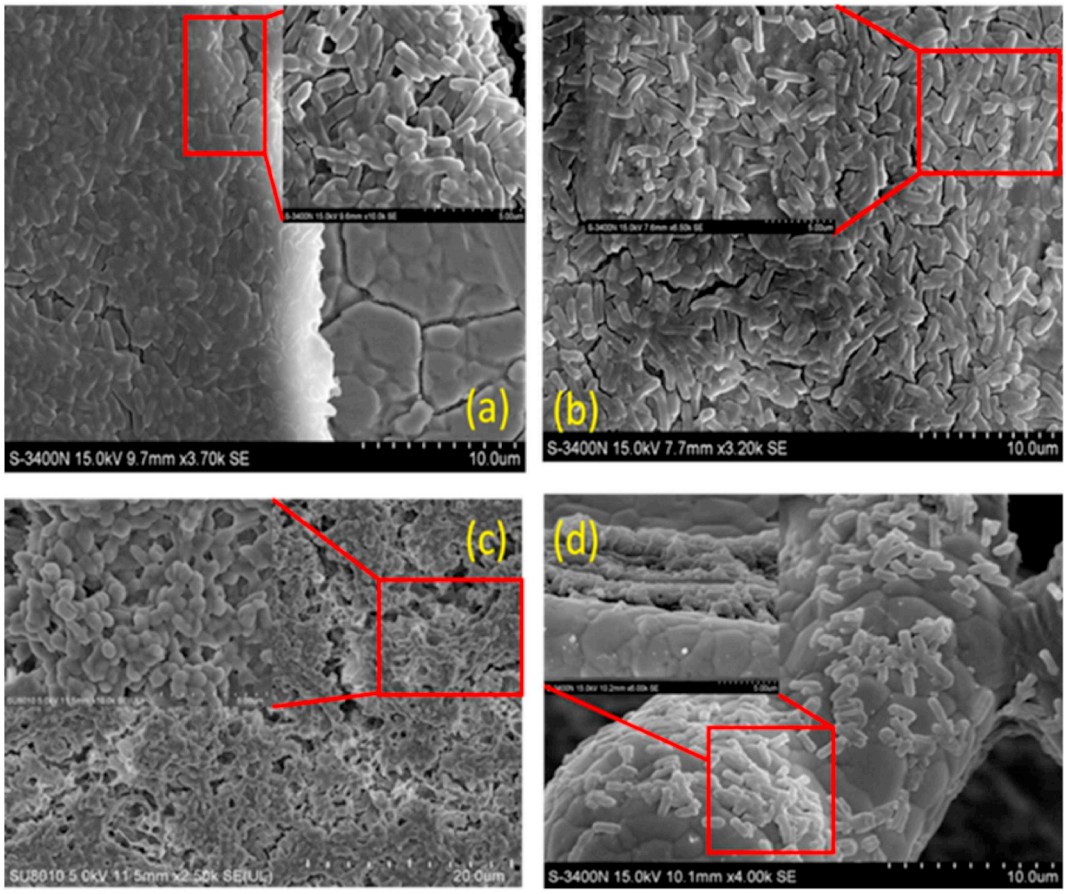

Fig. 2. SEM images of *E. coli* K-12 biofilm cultured onto (a) SS, (b) Ti, (c) Cu and (d) Ni substrates.

However, in this work, after a period of cultivation, the bacterial biofilms resumed growth. A possible reason for this is that bacterial cells suffered extensive membrane damage within minutes of being exposed to Cu surface, but the DNA was not immediately affected due to the protection of the periplasm (Grosse et al., 2014). That is, some bacteria were not completely killed, but were still in a slow-growing state.

To further understand the differences between the biofilms grown on these substrates, the morphology of mature biofilms was observed using SEM (Fig. 2). The morphology of bacteria on SS and Ti substrates were very similar (Fig. 2a and b). The biofilm bacteria gathered in a sheet form and the cells were closely connected with each other. A cross-sectional view showed that the biofilm consisted of multiple layers, each of which was arranged in close order. Comparatively, bacteria on Cu were short and round, and connected with a spherical shape (Fig. 2c), which was different from the long rod-shaped bacteria on SS and Ti substrates. In addition, instead of an orderly arrangement, like on SS and Ti substrates, the bacteria on Cu were condensed into clusters. On Ni substrate (Fig. 2d), due to its pore-like structure, the short rod-shaped bacteria were trapped into the voids, and the biofilm was distributed unevenly. A cross section showed that the bacteria were gathered to form a cylindrical one. It is reasonable to explain these changes in the physiological form of bacteria, since they are under some stress from adverse environments (Chen et al., 2018; Zhang et al., 2015). For instance, *E. coli* cells become shorter after chlorine and chloramine treatment (Chen et al., 2018).

3.2. Characteristic variation of EPS on different materials over time

As above-mentioned, EPS is an important biofilm component. To comprehend the characteristic variation of EPS during biofilm formation on different materials, the composition and production of EPS (total carbohydrate and protein) were further investigated (Figs. S7 and 3). EPS concentrations on SS substrate increased rapidly to the maximum (2847 μg/total cell, with 2037 and 810 μg/total cell for total carbohydrate and protein, respectively) within 72 h and then decreased gradually (Fig. S7a), which were in good agreement with the results of biofilm thickness (Fig. 1b). These results illustrated that EPS concentrations varied with the fluctuation of the total bacterial amount, leading to the change in biofilm thickness. Furthermore, EPS concentrations per cell were also analyzed (Fig. 3), showing a gradual increase with incubation time, and then a slight decrease after maturity (Fig. 3a), reaching a maximum concentration of 512 and 229 μg/10^8 cells for total carbohydrate and protein, respectively, within 64-h cultivation. Alterations in the EPS concentrations, when also considering the growth activity, suggested that the bacterial biofilm may not experience extreme damage upon exposure to SS surface.

Usually, the carbohydrate to protein ratio plays a significant role in monitoring the state of biofilm formation when biofilms are exposed to metal substrates (O'Loughlin and Chin, 2001). Specifically, the total carbohydrate content was 1–2 times that of the protein content (Fig. S8a). Moreover, the ratio of carbohydrate to protein first increased and then decreased. That is, more polysaccharides were secreted at early stage, while more protein was secreted at late stage, indicating that they may play unique roles at different biofilm development stages.

On Ti substrate, a similar trend in EPS concentrations was found during bacterial biofilm development process (Fig. S7b), with the maximum value (2438 μg/total cell) observed at 64 h. As compared with SS substrate, the change in EPS content was gentle and EPS concentration was slightly less (Figs. 3b and S8b), peaking at 502 and 227 μg/10^8 cells for total carbohydrate and protein, respectively, with a carbohydrate to protein ratio of 2.05. The ratio stayed relatively constant, suggesting that both play important roles in biofilm development.

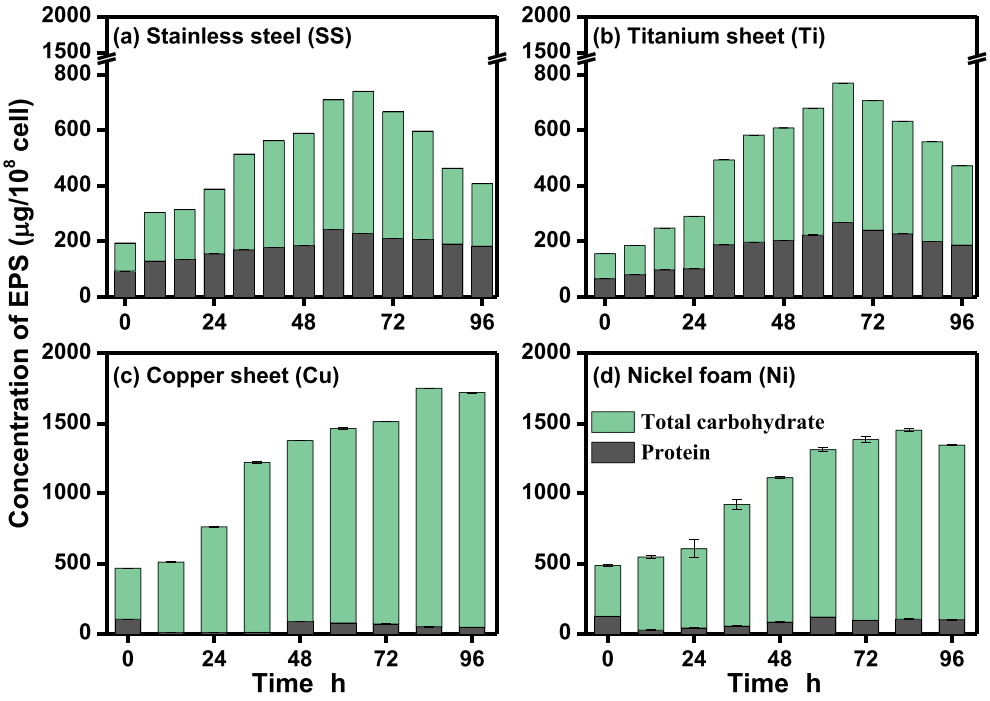

Fig. 3. The protein and total polysaccharide concentration of EPS extracted from *E. coli* K-12 biofilm growing onto (a) SS, (b) Ti, (c) Cu and (d) Ni substrates.

The possible reason for this will be discussed later by monitoring the molecular regulatory network.

Comparatively, the EPS concentrations on Cu and Ni substrates were much lower than those on SS and Ti substrates, with a minimum content of 14 and 40 μg, respectively, within 24–48-h cultivation (Figs. S7c and d), indicating that biofilms on these substrates were initially much thinner than those on SS and Ti. Furthermore, the EPS concentrations also decreased at the beginning, which was consistent with the change in the total bacterial number. Different from the response of bacteria on SS and Ti substrates, a strange phenomenon was observed on Cu. That is, the EPS concentration of biofilm on Cu surface increased dramatically at first, and then became much higher than that on SS and Ti substrates (Figs. 3c and S8c), especially the total carbohydrate. The highest carbohydrate to protein ratio was 64 after 24-h cultivation, due to a very low level of protein (8 μg/10^8 cells). This might be because a portion of bacteria were killed during biofilm development on Cu surface (Grosse et al., 2014). As such, total carbohydrate in the measured EPS may contain biological debris, which can be detected through filter membrane, showing a high level of carbohydrate. It is also important to consider that EPS is only restricted to be generated by biofilms (Perez and Susa, 2017), specifically bacteria suffering terrible conditions. Therefore, in this study, the protein content of measured EPS on Cu substrate was extremely low because of low bacterial cell number. Overall, bacteria were severely damaged, but exhibited a strong response to external threats under some special circumstances.

Similarly, EPS concentrations on Ni substrate reached the highest value at the beginning, with a low bacterial abundance but high carbohydrate level (Figs. 3d and S8d). However, carbohydrate concentrations of Ni biofilm were not as high as that on Cu, and protein concentration was still maintained at a normal level. According to a reference (Perez and Susa, 2017), the dynamic nature of EPS in biofilms depends on their requirements (including nutrition and protection). That is, although the exposure of bacteria to Ni can also inactivate them, the role of EPS could be different. Besides providing mechanical stability, mediating bacterial adhesion to surfaces and forming a cohesive biofilm, EPS could also provide nutrient absorption from water, thereby helping to maintain bacterial density (Flemming and Wingender, 2010).

3.3. Oxidative stress response during biofilm formation process on different substrates

3.3.1. ROS generation and anti-oxidative enzymatic activities

Numerous studies have reported that toxic doses of some metal ions, especially Fe(II) and Cu(II), can increase the intracellular ROS level and stimulate the bacterial oxidative stress response (Harrison et al., 2009; Warnes et al., 2012). During the biofilm development process, bacterial cells will inevitably interact with the substrate. Therefore, to investigate whether biofilm bacteria were oxidatively stressed during growth on these metallic materials and the response of the biofilm bacteria to the oxidation pressure, the intracellular ROS level and anti-oxidative enzyme activities were assayed during the biofilm growth period. On SS and Ti, the intracellular ROS levels slightly increased at the beginning and then fluctuated slightly (Fig. 4a). This indicates that oxidative stress responses indeed occurred in the biofilm bacteria, but the biofilms on both substrates were more tolerant of oxidation pressure and invariably maintained their redox equilibrium. To achieve this goal and maintain normal bacterial metabolic activity, the content of anti-oxidative enzymes, SOD, CAT and GHS-Px also slightly increased initially (Fig. 4b, c and d) and served as scavengers of ROSs to eliminate intracellular oxidative damage in the bacteria (Yin et al., 2019).

In contrast, intracellular ROSs within biofilm bacteria on Cu substrate increased obviously within the initial 2 days (Fig. 4a), indicating that intracellular oxidative stress was significantly aroused under this circumstance. Comparatively, the intracellular ROS levels within bacteria on Ni substrate were much higher than those on SS and Ti, but lower than that on Cu. Correspondingly, SOD, CAT and GHS-Px activities in the bacterial cells also increased rapidly when the bacteria contacted Cu and Ni substrates (Fig. 4b, c, d). Moreover, the antioxidant activities reached their highest levels within one or two days, while bacterial regrowth occurred after two days of sharp decline at the initial time (Fig. 1a). Previous studies reported that *E. coli* on solid Cu surfaces might be predominantly killed through membrane damage (Grosse et al., 2014) and that bacteria exposed to toxic doses of Cu(II) could upregulate genes involved in ROS elimination (Lemire et al., 2013). Hence, we assumed that Cu ions might be released from Cu substrate during the biofilm development process, and that toxicity associated

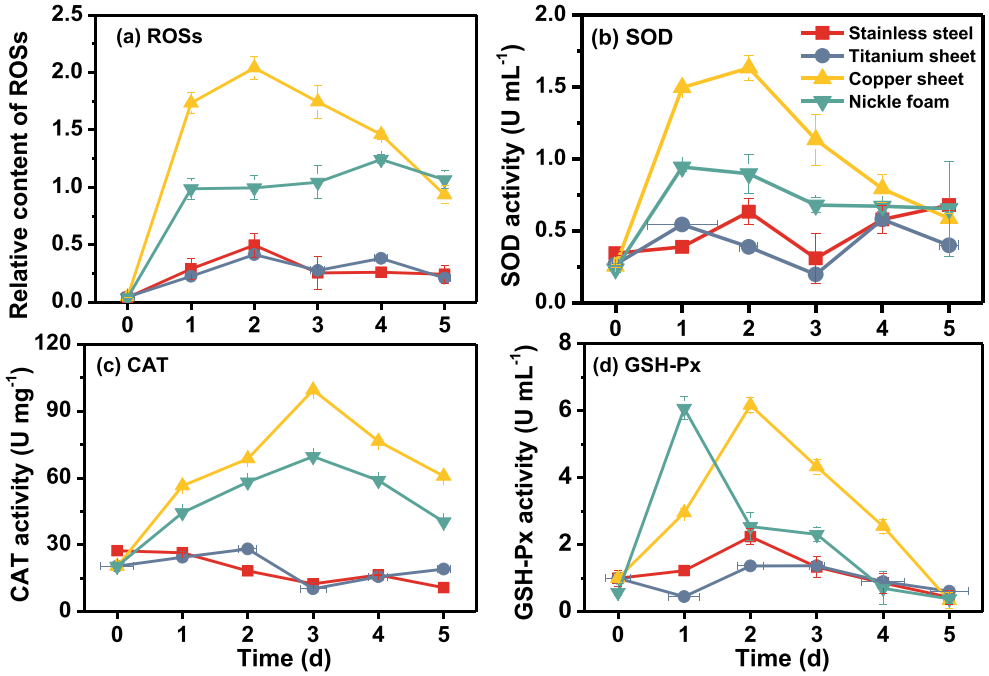

Fig. 4. (a) Intracellular ROSs level tested by DCFH-DA; (b) SOD activity and (c) CAT activity of biofilm onto SS, Ti, Cu, and Ni substrates during biofilm formation.

with Cu ions might be the cause of ROS-mediated cellular damage. Previous research reported that survival of *E. coli* cells on Cu surface increased by addition of glutathione (Grosse et al., 2014). However, here, the activities of all anti-oxidative enzymes, including GSH, increased during the intinal one or two days, which could not directly explain the special role of GSH in bacterial survival.

3.3.2. Gene expression of oxidative stress and metal transporter

To further confirm that biofilm bacteria produce oxidative stress on different metal substrates, and to clarify the interaction between biofilm bacteria and metals, the expression of genes related to oxidative stress and the metal transporter in the bacteria were examined in detail. The expression profiles of all tested genes are illustrated as a heat map (Fig. 5). On SS and Ti substrates, the expression of oxidative stress genes was slightly up-regulated by 1–2 folds after 2–3 days of cultivation. This result is almost consistent with the changes of anti-oxidative enzyme activities (Fig. 4b, c and d). Furthermore, with the increased anti-oxidative enzyme content, the involved stress genes were also slightly up-regulated, but there was no particularly prominent gene expression, indicating that oxidative stress is a collective response to external damage during this process. Moreover, no obvious change in the metal transporter-related genes was involved, indicating that no metal ions entered and exited the cell membrane during these processes. This result also agrees well with the increased bacterial abundance during the biofilm formation process, although some small adverse effects occurred during these processes (Fig. 1a1).

On Cu substrate, almost all tested genes were up-regulated 2–11 folds (Fig. 5) during biofilm development, which were much higher than those on SS and Ti substrates. This suggests that Cu may trigger stress-response mechanisms that protect cells in order to cope with external damage. In particular, the highly expressed *rpoS*, *oxyR*, *osmC* and *zupT* genes are coding proteins associated with general stress response (Somorin et al., 2017); surface proteins that control colony morphology and auto aggregation ability (Gundlacht and Winter, 2014); an osmotically inducible peroxiredoxin (Cussiol et al., 2010); and a metal transporter (Taudte and Grass, 2010), respectively. The Cu surface might be oxidized to Cu ions that then enter the cell through a metal transporter, causing an imbalance of intracellular redox and destruction of cell membrane permeability. Simultaneously, oxidative stress motivated the bacterial surface protein responses, resulting in changes of community morphology and bacterial aggregation ability. As observed from our above experiments, when bacteria contacted and grew on Cu substrate, most bacteria were instantly inactivated, as demonstrated by the sharp decrease in cell number (Fig. 1a), decrease in extracellular protein content (Figs. 3 and S8), alteration of cellular morphology (Fig. 2) and increase in intracellular ROSs and anti-oxidative enzyme activities (Fig. 4).

Compared with SS and Ti substrates, most of the tested genes were also up-regulated on Ni substrate (2–9 folds) (Fig. 5). Among them, higher expression was observed for the *rpoS* and *oxyR* genes, which encode proteins related to the general stress response, colony morphology and auto-aggregation ability control. This also indicates that the oxidative stress response of the biofilm bacteria on Ni substrate was triggered, which could account for the decreased bacterial growth. In addition, the expression of *zinT* gene, encoding metal-binding protein, was also slightly up-regulated (3.87 folds). This demonstrates that the metal-binding protein, zinT, may bind nickel ions to pose stress to bacteria (Kershaw et al., 2007). Furthermore, under the action of bacteria in nutrient solution, nickel is oxidized to nickel ions, which then binds with the binding protein, causing a series of oxidative stress responses as described above. To a lesser extent, Ni ions can catalyze Fenton reactions in vitro at a significantly slower rate (Lemire et al., 2013). Therefore, bacterial cells were less damaged on Ni than Cu substrates. This is shown by the fact that after adapting to Ni substrate, bacteria also began to proliferate and the biofilm developed quickly after the initial slight damage (Fig. 1a).

3.4. Molecular regulation network of biofilm development

To further explore the feedback mechanism of *E. coli* biofilms grown on four different metal substrates, the expression levels of genes related to flagella and motility, adhesive polysaccharides, signal proteins and quorum sensing were analyzed to determine their effect on the molecular regulatory network of the biofilm (Fig. 6).

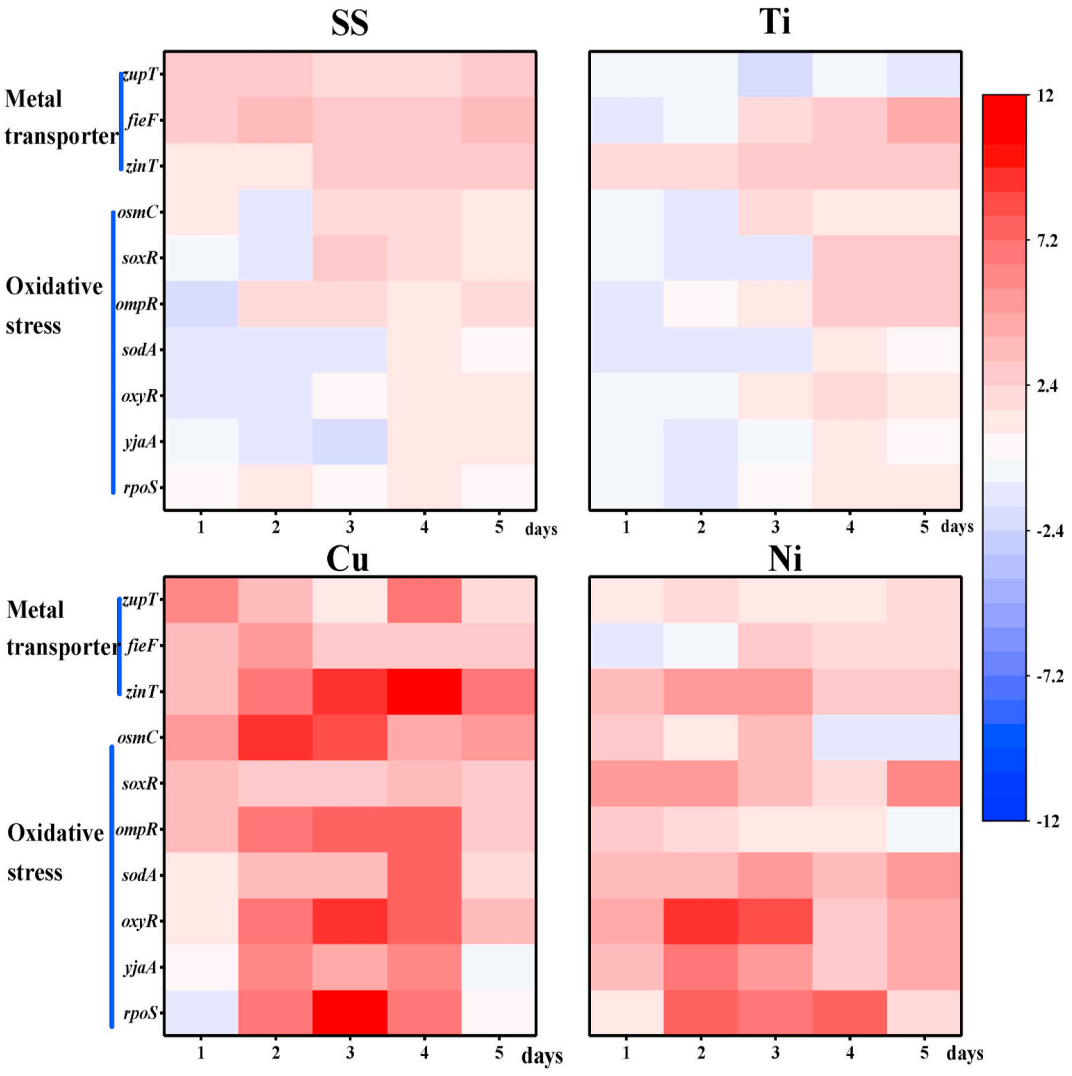

Fig. 5. Gene expression heatmap of target genes involved in oxidative stress regulation and metal transporter in *E. coli* K-12 cultured onto SS, Ti, Cu and Ni substrates. X-axis: the monitoring time in days; Y-axis left: clusters of target genes and list of genes tested, Y-axis right: the figure legend bar (depicted a blue-red color scale. Red spectrum color indicates up-regulated expression; green spectrum color indicated down-regulated expression). (For interpretation of the references to color in this figure legend, the reader is referred to the Web version of this article.)

3.4.1. Expression of genes related to flagella and motility

In the flagellum and motility mechanism system, the *motA* gene, encoding a motility protein (Blair and Berg, 1990), was up-regulated in the bacteria along with the growth of the biofilm. The highest up-regulation was 3.4 and 3.7 times and then down-regulated by 4.5 and 2.1 times after 4–5 days of cultivation on SS and Ti substrates, respectively. Additionally, the expression of the *BssR* gene, a regulator of biofilm formation (Ren et al., 2004), was slightly up-regulated by 1–4 times in bacteria on SS substrate and 1–3 times on Ti. Unlike *motA*, the expression of *glgS* gene, involved in glycogen biosynthesis and a negative regulator of motility (Rahimpour et al., 2013), was slightly down-regulated at the early stage and then up-regulated after 3 days of cultivation. These results indicate that biofilms on SS and Ti substrates are in different developmental processes. At early biofilm formation stage, the flagella gene (*motA*) was up-regulated, meaning that bacteria began to gather into clusters to form a biofilm, while at later stage when the biofilm was stable and the flagella were not needed, its expression was inhibited. Flagellum production and movement place a high energy burden on cells; thus, limiting their expression is conducive to glycogen production, which is beneficial to cell survival (Rahimpour et al., 2013). According to a reference, the generation of flagella and glycogen occurs in *E. coli* at exponential cell growth stage. However, the former mainly occurs at the early stage of exponential cell growth, while the latter mainly occurs during the transition from exponential growth to the stable period (Rahimpour et al., 2013).

On the contrary, the *motA* gene in bacteria on Cu substrate was down-regulated by 1–2 times at early cultivation stage, and then was gradually up-regulated by 3–4.5 times after 3 days of cultivation. An opposite trend was observed for *glgS* gene expression, while the *BssR* gene was slightly up-regulated by 1-2-fold during almost the whole period. For the biofilm on Ni substrate, the *motA* and *BssR* genes were maintained at 1–4 folds and 1–3 folds up-regulation, respectively. The *glgS* gene was up-regulated at early cultivation stage and then was gradually down-regulated (Fig. 6). This can be explained because the biofilm bacteria on Cu were vulnerable at the beginning and then stimulated to an active defense state. Usually, the expression of flagella and motility genes requires energy consumption, which will be inhibited if the bacteria are in a defense state (Rahimpour et al., 2013). These genes were then up-regulated as the surviving bacteria grew. Comparatively, bacteria on Ni substrate suffered less damage. Therefore, the inhibition on Ni substrate was less than that on Cu substrate, although the flagella and motor genes were also inhibited at early stage. Subsequently, as the bacteria gradually adapted, these genes began to be expressed during biofilm development.

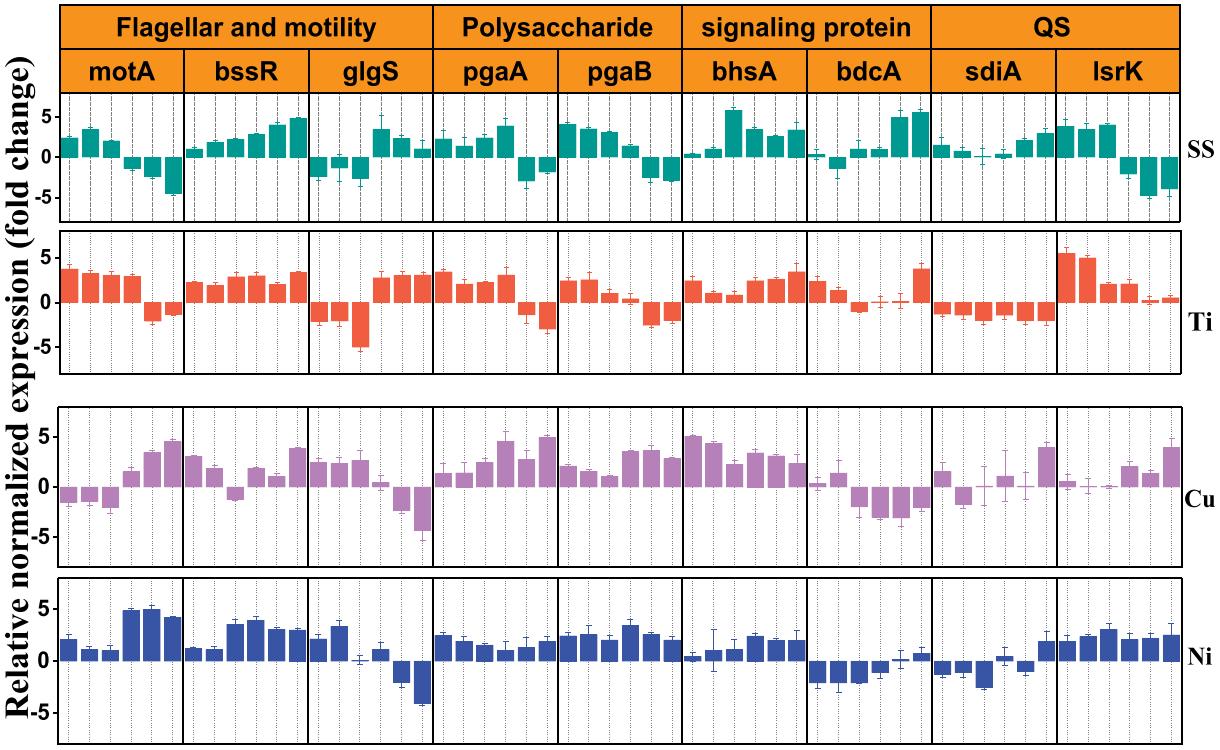

Fig. 6. Gene expression profiles of target genes involved in adhesin polysaccharide, flagellar and motility, QS system and signaling protein in *E. coli* K-12 biofilm.

3.4.2. Expression of genes related to adhesive polysaccharide

Poly-β-1,6-N-acetyl-$_D$-glucosamine (β-1,6-GlcNAc; PGA), an adhesin polysaccharide involved in biofilm formation, maintains the stability of the bacterial biofilm structure and requires the genetic products of the pgaABCD operon to perform its function (Itoh et al., 2008). Therefore, the expression of the *pgaA* and *pgaB* genes in the biofilm bacteria was also analyzed (Fig. 6). On SS and Ti substrates, both genes were slightly up-regulated by 1–3 folds at early stage and then down-regulated by 1–2 folds after 3–4 days of cultivation. These results demonstrate that on SS and Ti substrates, exopolysaccharide secretion increased at early stage of the biofilm development but decreased at late stage. All these phenomena were consistent with the results of EPS analysis (Fig. 3) and accounted for the ratio variation over time (Fig. S8).

Comparatively, the expression of polysaccharide genes on Cu substrate increased 1–4 times during the whole biofilm formation process, whereas expression on Ni substrate slightly increased with some fluctuation (Fig. 6). These results showed that exopolysaccharide secretion increased during the whole culture process on Cu and Ni substrates; in particular, the carbohydrate concentration increased significantly in the EPS (Fig. 3). Combined with the oxidative stress results (Figs. 4 and 5), we inferred that the dramatic increase in EPS carbohydrates was due to dead cells leaving the extracellular matrix.

3.4.3. Expression of genes related to signal proteins and quorum sensing (QS)

A previous study showed that *BhsA* is significantly induced in *E. coli* biofilms as well as by some adverse stress conditions, such as exposure to acid, heat, H_2O_2 and cadmium (Zhang et al., 2007). Thus, the *bhsA* gene (encoding an outer membrane protein) was also minitored in this work, and was also found to be up-regulated in the biofilm bacteria on all four substrates throughout the entire biofilm development process (Fig. 6). That is, when biofilm bacteria grew on metal substrates, they encountered some adverse stress, subsequently inducing the up-regulation of the *bhsA* gene. Additionally, expression of other stress related genes can be simultaneously induced (Fig. 5). As a result, bacterial biofilms were successfully developed on all four metal substrates by ultimately protecting themselves from the toxcitity of metal ions, despite much higher intense stress from the Cu and Ni substrates.

Another gene related to signal protein, *bdcA*, which mainly regulates biofilm diffusion by decreasing the concentration of cyclic di-guanylate monophosphate (c-di-GMP), is an intracellular messenger that controls cell motility via flagellar rotation and biofilm formation through synthesis of curli and cellulose (Ranjith et al., 2019). In this study, no significant change was observed for *bdcA* gene expression until it was up-regulated by 3.7–5.57 folds during the final day one or two of cultivation on SS and Ti substrates. Up-regulation of the *bdcA* gene indicates that biofilm development was at the shedding stage, during which the bacteria begin to disperse, and the biofilm gradually falls off. Meanwhile, the aggregation of cells and EPS concentration both decreased (Figs. 1 and S7). However, the *bdcA* gene was down-regulated by 1–2 folds on Cu and Ni substrates during the whole process, indicating that shedding and dispersion of the biofilms was not initiated. Considering the sudden decrease of bacterial number at early growth stage and the increasing concentration of polysaccharides, we can infer that bacteria on Cu and Ni substrates encountered threats to some extent. Simultaneously, the biofilm shedding-related genes should be inhibited and the *bhsA* gene should be down-regulated.

Several mechanisms of *E. coli* are regulated by QS, which is a signaling system that enables bacteria to respond to chemical molecules known as autoinducers, including virulence factors and biofilm formation (Culler et al., 2018). The suppressor of division inhibitor (SdiA) is a QS receptor present in *E. coli* that plays an important role in the regulation of biofilms and biofilm-related structures when the bacteria experience stress (Lee et al., 2009). In this study, at initial biofilm development stage, no significant change was observed in the expression of the QS-related gene *sdiA*; however, it was eventually up-regulated by 2 fold on SS substrate. Comparatively, a fixed 2-fold down-regulation was observed on Ti substrate, suggesting that this gene was expressed stably during the biofilm development process. Similarly, on Cu and Ni substrates, the gene expression level fluctuated between 1 and 2 times down-regulation. According to Culler et al. SdiA can inhibit biofilm formation and adhesion to surfaces (Culler et al., 2018). Therefore, in

this study, at early biofilm development stage, bacterial abundance and polysaccharide secretion increased, at which sdiA as an inhibitor should be suppressed. On the other hand, when bacteria are under stress conditions, such as low nutrient availability, temperature changes and other stress related factors, sdiA is inhibited, thereby alleviating the repressor effect on the expression of these genes, leading to biofilm development (Van Houdt et al., 2006). As such, considering the enhanced oxidative stress response of bacteria on Cu and Ni substrates, the bacteria are indeed attacked by metal ions, leading to inhibition of *sdiA* gene expression and subsequent biofilm formation.

Conversely, the *lsrK* gene on SS and Ti substrates was up-regulated along with biofilm growth, with the highest up-regulation by 4.0 and 5.4 times, respectively, followed by a down-regulation by 4.7 and 0.22 times, respectively, after 3–4 days of cultivation. As reported, *lsrK* encodes an AI-2 (automatic-inducer) kinase, which produces phosphorylated AI-2, enabling cells to sense and communicate with each other (Xavier et al., 2007). In this study, the amount of AI-2 kinase increased and accumulated during the growth of biofilms and then began to decline rapidly after biofilm maturation, which agrees with other reports (Rahimpour et al., 2013; Xiao et al., 2016). In contrast, obvious variation of the *lsrK* gene was observed on Cu substrate till a 2–4.9-fold up-regulation after 3 days of cultivation. Nevertheless, there was a fixed fluctuation range from 2.2 to 3.0-fold for the *lsrK* gene on Ni substrate, indicating that the amount of AI-2 secreted by bacteria on this substrate maintained a fluctuating equilibrium level. Similarly, the up-regulation of AI-2 kinase activates AI-2 signaling molecules and bacterial aggregation facilitates the formation of biofilms. This indicates that bacteria on Cu and Ni substrates survived oxidative stress and began to develop a biofilm, which is an emergent form of bacterial life.

Overall, the bacterial growth activity of biofilms is not same on different metal substrates, and the biofilms at the same culture stage are in different biofilm development stages. During the growth period, flagella and polysaccharide genes were activated and expressed to facilitate secretion of extracellular substances and enhance bacterial adhesion. During the growth and stabilization period, the expression of QS- and signal protein-related genes were up-regulated to aggregate cells. During the later stabilization period, signaling molecule-related genes that affect the c-di-GMP pathway were up-regulated to guide the dispersion and shedding of bacteria.

4. Conclusion

This study demonstrated that biofilm bacteria could inhabit different metal substrates and exhibit distinct feedbacks due to various degrees of stress. When planktonic bacteria directly contact with Cu and Ni substrate surfaces, their activity drops sharply. This is manifested by a lower bacterial abundance, altered cellular morphology and sudden increase in carbohydrate content in EPS, as compared with those on SS and Ti substrates. Furthermore, due to the destruction of the bacterial redox equilibrium, bacteria on Cu substrate have the most active and drastic defense, followed by those on Ni substrate. Moreover, bacteria can quickly adapt to SS and Ti substrates to form biofilms while the surviving bacteria on Cu and Ni substrates also aggregate to develop biofilms to protect internal cells from adverse external damage. Ultimately, these behaviors are performed under the biofilm regulatory molecular network. This study revealed the response and underlying mechanisms of bacterial biofilm development on different metal substrates. As such, this information provides a better understanding of different strategies pursued by bacteria during biofilm colonization on different metal-based pipelines in water distribution systems, which has implications for the control and elimination of biofilm contamination.

Declaration of competing interest

The authors declare that they have no known competing financial interests or personal relationships that could have appeared to influence the work reported in this paper.

Acknowledgements

This work was supported by the National Natural Science Foundation of China (41573086, 41425015 and U1901210) and Science and Technology Project of Guangdong Province, China (2017A050506049).

Appendix A. Supplementary data

Supplementary data to this article can be found online at https://doi.org/10.1016/j.envres.2020.109451.

References

Azeredo, J., Azevedo, N.F., Briandet, R., Cerca, N., Coenye, T., Costa, A.R., Desvaux, M., Di Bonaventura, G., Hebraud, M., Jaglic, Z., Kacaniova, M., Knochel, S., Lourenco, A., Mergulhao, F., Meyer, R.L., Nychas, G., Simoes, M., Tresse, O., Sternberg, C., 2017. Critical review on biofilm methods. Crit. Rev. Microbiol. 43 (3), 313–351.

Blair, D.F., Berg, H.C., 1990. The MotA protein of *E. coli* is a proton-conducting component of the flagellar motor. Cell 60 (3), 439–449.

Buse, H.Y., Ji, P., Gomez-Alvarez, V., Pruden, A., Edwards, M.A., Ashbolt, N.J., 2017. Effect of temperature and colonization of *Legionella pneumophila* and *Vermamoeba vermiformis* on bacterial community composition of copper drinking water biofilms. Microb. Biotechnol. 10 (4), 773–788.

Chen, S., Li, X., Wang, Y., Zeng, J., Ye, C., Li, X., Guo, L., Zhang, S., Yu, X., 2018. Induction of *Escherichia coli* into a VBNC state through chlorination/chloramination and differences in characteristics of the bacterium between states. Water Res. 142, 279–288.

Chen, X., Yin, H., Li, G., Wang, W., Wong, P.K., Zhao, H., An, T., 2019. Antibiotic-resistance gene transfer in antibiotic-resistance bacteria under different light irradiation: implications from oxidative stress and gene expression. Water Res. 149, 282–291.

Culler, H.F., Couto, S.C.F., Higa, J.S., Ruiz, R.M., Yang, M.J., Bueris, V., Franzolin, M.R., Sircili, M.P., 2018. Role of SdiA on biofilm formation by atypical enteropathogenic *Escherichia coli*. Genes 9 (5), 253.

Cussiol, J.R.R., Alegria, T.G.P., Szweda, L.I., Netto, L.E.S., 2010. Ohr (organic hydroperoxide resistance protein) possesses a previously undescribed activity, lipoyl-dependent peroxidase. J. Biol. Chem. 285 (29), 21943–21950.

Flemming, H.C., Wingender, J., 2010. The biofilm matrix. Nat. Rev. Microbiol. 8 (9), 623–633.

Flemming, H.C., Wingender, J., Szewzyk, U., Steinberg, P., Rice, S.A., Kjelleberg, S., 2016. Biofilms: an emergent form of bacterial life. Nat. Rev. Microbiol. 14 (9), 563–575.

Grosse, C., Schleuder, G., Schmole, C., Nies, D.H., 2014. Survival of *Escherichia coli* cells on solid copper surfaces is increased by glutathione. Appl. Environ. Microbiol. 80 (22), 7071–7078.

Gundlacht, J., Winter, J., 2014. Evolution of *Escherichia coli* for maximum HOCl resistance through constitutive expression of the OxyR regulon. Microbiology 160, 1690–1704.

Hall-Stoodley, L., Costerton, J.W., Stoodley, P., 2004. Bacterial biofilms: from the natural environment to infectious diseases. Nat. Rev. Microbiol. 2 (2), 95–108.

Harrison, J.J., Tremaroli, V., Stan, M.A., Chan, C.S., Vacchi-Suzzi, C., Heyne, B.J., Parsek, M.R., Ceri, H., Turner, R.J., 2009. Chromosomal antioxidant genes have metal ion-specific roles as determinants of bacterial metal tolerance. Environ. Microbiol. 11 (10), 2491–2509.

Isaac, T.S., Sherchan, S.P., 2020. Molecular detection of opportunistic premise plumbing pathogens in rural Louisiana's drinking water distribution system. Environ. Res. 181 108847.

Itoh, Y., Rice, J.D., Goller, C., Pannuri, A., Taylor, J., Meisner, J., Beveridge, T.J., Preston III, J.F., Romeo, T., 2008. Roles of pgaABCD genes in synthesis, modification, and export of the *Escherichia coli* biofilm adhesin poly-beta-1,6-N-acetyl-D-glucosamine. J. Bacteriol. 190 (10), 3670–3680.

Jungfer, C., Friedrich, F., Villarreal, J.V., Brandle, K., Gross, H.J., Obst, U., Schwartz, T., 2013. Drinking water biofilms on copper and stainless steel exhibit specific molecular responses towards different disinfection regimes at waterworks. Biofouling 29 (8), 891–907.

Kershaw, C.J., Brown, N.L., Hobman, J.L., 2007. Zinc dependence of zinT (yodA) mutants and binding of zinc, cadmium and mercury by ZinT. Biochem. Biophys. Res. Commun. 364 (1), 66–71.

Lee, J., Maeda, T., Hong, S.H., Wood, T.K., 2009. Reconfiguring the quorum-sensing regulator SdiA of *Escherichia coli* to control biofilm formation via indole and n-acylhomoserine lactones. Appl. Environ. Microbiol. 75 (6), 1703–1716.

Lee, W.H., Pressman, J.G., Wahman, D.G., 2018. Three-dimensional free chlorine and monochloramine biofilm penetration: correlating penetration with biofilm activity and viability. Environ. Sci. Technol. 52 (4), 1889–1898.

Lemire, J.A., Harrison, J.J., Turner, R.J., 2013. Antimicrobial activity of metals: mechanisms, molecular targets and applications. Nat. Rev. Microbiol. 11 (6), 371–384.

Lewis, K., 2007. Persister cells, dormancy and infectious disease. Nat. Rev. Microbiol. 5 (1), 48–56.
Li, G., Chen, X., Yin, H., Wang, W., Wong, P.K., An, T., 2020. Natural sphalerite nanoparticles can accelerate horizontal transfer of plasmid-mediated antibiotic-resistance genes. Environ. Int. 136, 105497.
Liu, S., Gunawan, C., Barraud, N., Rice, S.A., Harry, E.J., Amal, R., 2016. Understanding, monitoring, and controlling biofilm growth in drinking water distribution systems. Environ. Sci. Technol. 50 (17), 8954–8976.
Markova, J.A., Anganova, E.V., Turskaya, A.L., Bybin, V.A., Savilov, E.D., 2018. Regulation of *Escherichia coli* biofilm formation. Appl. Biochem. Microbiol. 54 (1), 1–11.
Nakano, D., Strayer, D.L., 2014. Biofouling animals in fresh water: biology, impacts, and ecosystem engineering. Front. Ecol. Environ. 12 (3), 167–175.
O'Loughlin, E., Chin, Y.P., 2001. Effect of detector wavelength on the determination of the molecular weight of humic substances by high-pressure size exclusion chromatography. Water Res. 35 (1), 333–338.
O'Toole, G.A., Pratt, L.A., Watnick, P.I., Newman, D.K., Weaver, V.B., Kolter, R., 1999. In: Doyle, R.J. (Ed.), Methods in Enzymology. Elsevier Inc, pp. 91–109.
Perez, M.F.L., Susa, M.R., 2017. Exopolymeric substances from drinking water biofilms: dynamics of production and relation with disinfection by products. Water Res. 116, 304–315.
Proctor, C.R., Dai, D., Edwards, M.A., Pruden, A., 2017. Interactive effects of temperature, organic carbon, and pipe material on microbiota composition and *Legionella pneumophila* in hot water plumbing systems. Microbiome 5. https://doi.org/10.1186/s40168-017-0348-5.
Rahimpour, M., Montero, M., Almagro, G., Viale, A.M., Sevilla, A., Canovas, M., Munoz, F.J., Baroja-Fernandez, E., Bahaji, A., Eydallin, G., Dose, H., Takeuchi, R., Mori, H., Pozueta-Romero, J., 2013. GlgS, described previously as a glycogen synthesis control protein, negatively regulates motility and biofilm formation in *Escherichia coli*. Biochem. J. 452, 559–573.
Ranjith, K., Ramchiary, J., Prakash, J.S.S., Arunasri, K., Sharma, S., Shivaji, S., 2019. Gene targets in ocular pathogenic *Escherichia coli* for mitigation of biofilm formation to overcome antibiotic resistance. Front. Microbiol. 10. https://doi.org/10.3389/fmicb.2019.01308.
Ren, D., Bedzyk, L.A., Thomas, S.M., Ye, R.W., Wood, T.K., 2004. Gene expression in *Escherichia coli* biofilms. Appl. Microbiol. Biotechnol. 64 (4), 515–524.
Ren, H.X., Wang, W., Liu, Y., Liu, S., Lou, L.P., Cheng, D.Q., He, X.F., Zhou, X.Y., Qiu, S.D., Fu, L.S., Liu, J.Q., Hu, B.L., 2015. Pyrosequencing analysis of bacterial communities in biofilms from different pipe materials in a city drinking water distribution system of East China. Appl. Microbiol. Biotechnol. 99 (24), 10713–10724.
Santo, C.E., Lam, E.W., Elowsky, C.G., Quaranta, D., Domaille, D.W., Chang, C.J., Grass, G., 2011. Bacterial killing by dry metallic copper surfaces. Appl. Environ. Microbiol. 77 (3), 794–802.
Shivapooja, P., Wang, Q.M., Orihuela, B., Rittschof, D., Lopez, G.P., Zhao, X.H., 2013. Bioinspired surfaces with dynamic topography for active control of biofouling. Adv. Mater. 25 (10), 1430–1434.
Somorin, Y., Bouchard, G., Gallagher, J., Abram, F., Brennan, F., O'Byrne, C., 2017. Roles for RpoS in survival of *Escherichia coli* during protozoan predation and in reduced moisture conditions highlight its importance in soil environments. FEMS Microbiol. Lett. 364 (19). https://doi.org/10.1093/femsle/fnx198.
Stewart, P.S., Franklin, M.J., 2008. Physiological heterogeneity in biofilms. Nat. Rev. Microbiol. 6 (3), 199–210.
Stone, M.R.L., Butler, M.S., Phetsang, W., Cooper, M.A., Blaskovich, M.A.T., 2018. Fluorescent antibiotics: new research tools to fight antibiotic resistance. Trends Biotechnol. 36 (5), 523–536.
Sun, H., Li, G., An, T., Zhao, H., Wong, P.K., 2016. Unveiling the photoelectrocatalytic inactivation mechanism of *Escherichia coli*: convincing evidence from responses of parent and anti-oxidation single gene knockout mutants. Water Res. 88, 135–143.
Sun, H., Li, G., Nie, X., Shi, H., Wong, P.K., Zhao, H., An, T., 2014. Systematic approach to in-depth understanding of photoelectrocatalytic bacterial inactivation mechanisms by tracking the decomposed building blocks. Environ. Sci. Technol. 48 (16), 9412–9419.
Taudte, N., Grass, G., 2010. Point mutations change specificity and kinetics of metal uptake by ZupT from *Escherichia coli*. Biometals 23 (4), 643–656.
Tolker-Nielsen, T., Sternberg, C., Clifton, N.J., 2014. Methods in Molecular Biology. Humana Press, New York, NY, pp. 615–629.
Van Houdt, R., Aertsen, A., Moons, P., Vanoirbeek, K., Michiels, C.W., 2006. N-acyl-L-homoserine lactone signal interception by *Escherichia coli*. FEMS Microbiol. Lett. 256 (1), 83–89.
Vlamakis, H., Chai, Y., Beauregard, P., Losick, R., Kolter, R., 2013. Sticking together: building a biofilm the *Bacillus subtilis* way. Nat. Rev. Microbiol. 11 (3), 157–168.
Warnes, S.L., Caves, V., Keevil, C.W., 2012. Mechanism of copper surface toxicity in *Escherichia coli* O157:H7 and *Salmonella* involves immediate membrane depolarization followed by slower rate of DNA destruction which differs from that observed for Gram-positive bacteria. Environ. Microbiol. 14 (7), 1730–1743.
Xavier, K.B., Miller, S.T., Lu, W., Kim, J.H., Rabinowitz, J., Pelczer, I., Semmelhack, M.F., Bassler, B.L., 2007. Phosphorylation and processing of the quorum-sensing molecule autoinducer-2 in enteric bacteria. ACS Chem. Biol. 2 (2), 128–136.
Xiao, X., Zhu, W.W., Liu, Q.Y., Yuan, H., Li, W.W., Wu, L.J., Li, Q., Yu, H.Q., 2016. Impairment of biofilm formation by TiO_2 photocatalysis through quorum quenching. Environ. Sci. Technol. 50 (21), 11895–11902.
Yin, H., Chen, X., Li, G., Chen, Y., Wang, W., An, T., Wong, P.K., Zhao, H., 2019. Sublethal photocatalysis bactericidal technology cause longer persistence of antibiotic-resistance mutant and plasmid through the mechanism of reduced fitness cost. Appl. Catal. B Environ. 245, 698–705.
Zhang, S.H., Ye, C.S., Lin, H.R., Lv, L., Yu, X., 2015. UV Disinfection induces a VBNC state in *Escherichia coli* and *Pseudomonas aeruginosa*. Environ. Sci. Technol. 49 (3), 1721–1728.
Zhang, X.S., Garcia-Contreras, R., Wood, T.K., 2007. YcfR (BhsA) influences *Escherichia coli* biofilm formation through stress response and surface hydrophobicity. J. Bacteriol. 189 (8), 3051–3062.